Probabilistic Weapon Engagement Zones

Grant Stagg[1] and Cameron K. Peterson[1]

***Abstract*— In this work, we present linearized probabilistic weapon engagement zones (linearized PEZ), which provide a method to prevent agents from engaging in a pursuer-evasion differential game while accounting for uncertainty in the parameters of the game. This type of differential game is commonly used to model adversarial environments, where the parameters of the adversary (pursuer), such as initial positions and range, are often unknown or uncertain. Additionally, with the increasing potential of GPS jamming in modern warfare, even friendly (evader) parameters, such as position and orientation, can be uncertain. We demonstrate that linearized PEZ effectively approximates the true engagement zone distribution found using a Monte Carlo method. Using linearized PEZ, we develop a path optimization algorithm that plans safe trajectories while addressing this uncertainty. Numerical simulations are presented to demonstrate the effectiveness of our approach.**

I. Introduction

Many navigation missions require traversing contested or adversarial environments, where the risk of exposure to threats is high. For example, a reconnaissance unmanned aerial vehicle (UAV) may need to navigate through enemy territory while minimizing its risk of detection or attack. Planning safe and efficient paths in such environments is crucial for mission success [1], [2]. Ideally, these paths would allow the UAV to traverse the region without the need for sudden evasive maneuvers. However, contested environments often involve adversaries with unknown or uncertain parameters, making the task more challenging. Effective planning algorithms must account for this uncertainty to ensure that the trajectories are safe.

We model our adversarial environments using engagement zones (EZ). EZs are regions that an agent cannot occupy if they want to avoid being neutralized by an enemy [3]. They are defined using the parameters of the enemy agents in the environment; adversary's speed, range, capture radius, etc. Past research has used cardiod shapes to define deterministic EZs [3]–[5]. In [3], the authors provide an optimal control strategy to guide a Dubins vehicle around a single cardoid-shaped EZ. Their work assumes that the parameters of the EZ are known (the size and location of the EZ), and they do not account for the uncertainty inherent in adversarial environments. Their work was extended to account for multiple deterministic EZs [4], and dynamic EZs, where the origin of the EZ changes over time [5]. All these works depend on knowing the parameters of the EZ precisely and do not account for uncertainty.

[1] G. Stagg and C. Peterson are with the Department of Electrical and Computer Engineering, Brigham Young University, Provo, UT, USA ggs24@byu.edu

Instead of using cardiod-shaped EZs, recent research has defined basic EZs (BEZs) using the geometric properties of differential games [6], which are frequently used to model adversarial threats [7]. A differential game is described by a set of differential equations and objectives for each player in the game. BEZs defined using differential games are more meaningful than cardiod-shaped EZs because they are tied to a specific model and represent the capabilities of the players in the game.

In this work, we consider the pursuit-evasion differential game, where the goal of the evader is to avoid capture by the pursuer. This game is described in detail in [8]. The authors in [6] use geometric properties of the pursuit-evasion differential game to define a BEZ: a zone where, if the evader continues on its current heading, it will be neutralized by the pursuer. Using the BEZ as a constraint for path planning prevents the evader from entering a region where they would need to engage in a pursuit-evader differential game. This definition of a BEZ depends on knowing the starting location of the pursuer, as well as its maximum speed, range, and capture radius. It also assumes that the evader's speed, heading, and global location are known. In contested environments, evaders often do not have access to this information and may instead have estimates or prior beliefs about these parameters. We develop linearized PEZ using the BEZ model to account for the uncertainty in these estimates or beliefs.

Other research on path planning in uncertain adversarial environments includes using stochastic differential games [9], [10]. The authors in [10] use path integral control, a sampling-based method, to solve zero-sum stochastic differential games. However, this work relies on a random sampling method that requires high-performance parallel computing to run in real time. In addition, these works guide the players of the game on what to do when the game has already started. BEZs provide the evader with information on where to navigate to avoid conflict altogether.

Instead of modeling the adversarial environment using differential games, researchers in [11] and [12] use radar probability of detection. They used a linearization technique to account for uncertainty in enemy radar's global location and power parameters. They then used the resulting model to plan safe paths that avoid radar detection. Their method only applies to avoiding detection by a radar system. Our approach uses the evader/pursuer differential game and could potentially be applied to a wider range of adversarial environments.

In this work, we extend the results of [6] by incorporating uncertainty in the location and headings of the

evader and the location, range, and capture radius of the pursuer. This is achieved through a linear sensitivity analysis of the engagement zone (EZ) equations presented in [6], focusing specifically on the case of a fast pursuer (where the speed of the pursuer is greater than the evader's speed). We provide a random sampling-based Monte Carlo PEZ method that accounts for uncertainty by generating many random samples. This serves as a baseline non-linear comparison for our linearized PEZ approach. Additionally, we present a B-Spline-based path planning algorithm that can incorporate the pursuer's and evader's uncertain parameters and provide safe paths for the evader to follow. This path-planning approach and the application of linearized PEZs are validated using Monte Carlo (MC) simulations.

The contributions of this paper are summarized as follows:

1) We provide a method to prevent agents from engaging in differential games while accounting for uncertainty in the parameters of a pursuit-evader differential game by linearizing the BEZ equations to create linearized PEZs.
2) We evaluate the PEZs using a Monte Carlo non-linear PEZ comparison.
3) We present a path planning algorithm that uses PEZs to find paths for the agent with a low probability of being neutralized, and use Monte Carlo simulations to validate the safety of our planning algorithms.

The remainder of the paper proceeds as follows. Background information on BEZs is found in Section II. Section III outlines our method for finding the linearized PEZs. Section IV shows how linearized PEZ can be used to plan safe trajectories. Simulation results are shown in Section V. Finally, conclusions are given in Section VI.

II. Background

BEZs are defined analytically using differential games. Because our algorithm operates from the perspective of the evader, we will refer to the evader as the agent. For the evader/pursuer case, the differential game is defined with dynamics for the agent and pursuer as

$$\dot{\boldsymbol{x}} = \begin{bmatrix} \dot{\boldsymbol{x}}_P \\ \dot{\boldsymbol{x}}_A \end{bmatrix} = \begin{bmatrix} \dot{x}_P \\ \dot{y}_P \\ \dot{x}_A \\ \dot{y}_A \end{bmatrix} = \begin{bmatrix} v_P \cos\psi_P \\ v_P \sin\psi_P \\ v_A \cos\psi_A \\ v_A \sin\psi_A \end{bmatrix}, \boldsymbol{x}(0) = \begin{bmatrix} \boldsymbol{x}_P(0) \\ \boldsymbol{x}_A(0) \end{bmatrix}, \tag{1}$$

where $\boldsymbol{x}_P$ is the pursuer's location, $\boldsymbol{x}_A$ is the agent's (evader's) location, v_P is the pursuer's speed, v_A is the agent's speed, ψ_P is the pursuer's heading and ψ_A is the agent's heading. The agent is neutralized if it comes within a capture radius r of the pursuer. The pursuer is considered range-limited (i.e., fuel/time limit), with maximum range R. Additionally, we define the speed ratio between the agent and the pursuer as $\nu = v_A/v_P$. This differential game is depicted in Figure 1.

The BEZ is defined as the region where the agent will be neutralized by the pursuer on a collision course if the agent doesn't deviate from it current trajectory or try to evade

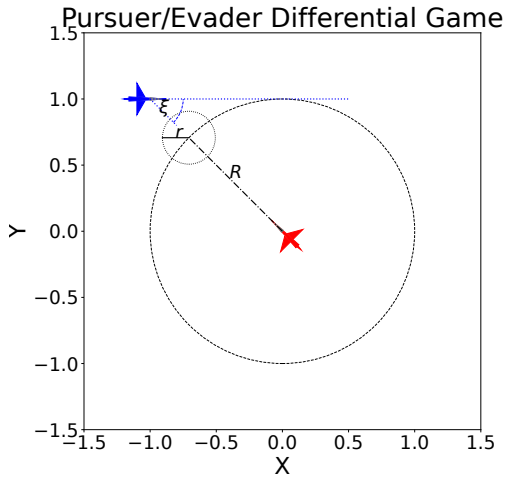

Fig. 1. This figure shows the evader/pursuer differential game. The pursuer (red) starts at the origin and has a finite range R. It neutralizes the agent if the agent/evader (blue) comes inside its capture radius r. The aspect angle ξ, is the angle between the heading of the agent and the line of sight direction of the pursuer.

the pursuer. This is more conservative than win/lose regions defined using solutions to the differential games as it does not require the agent to make evasive maneuvers to avoid capture. BEZs define a method for preventing the evader from ever entering a region where it would engage in the game.

The BEZ can be defined using the parameters of the differential game as [6]

$$\mathcal{Z} = \{\boldsymbol{x}_A : \|\boldsymbol{x}_A - \boldsymbol{x}_P(0)\|_2 \leq \rho(\xi, \nu, R, r)\}. \tag{2}$$

The function $\rho(\xi, \nu, R, r)$ can be found geometrically using the law of cosines for the case where $v_P > v_A$. For this fast pursuer ν is [6]

$$\rho(\xi, \nu, R, r) = \nu r \left(\cos(\xi) + \sqrt{\cos^2(\xi) - 1 + \frac{(R+r)^2}{\nu^2 R^2}} \right), \tag{3}$$

where ξ is the aspect angle between the agent's heading and the pursuer defined as

$$\xi(\boldsymbol{x}_A, \boldsymbol{x}_P(0)) = \psi_A - \arctan\left(\frac{y_P(0) - y_A}{x_P(0) - x_A} \right). \tag{4}$$

The BEZ defines a region where the agent will be caught if it keeps its same heading and, therefore, changes depending on the heading of the agent. This means that an agent's engagement zone is constantly evolving as an agent moves along its trajectory. Using BEZs, as defined above, allows path-planning algorithms to find safe trajectories that guarantee they will not be captured and do not require evasive maneuvers.

III. Probabilistic Weapon Engagement Zones

The BEZ model requires the agent to know its own parameters: position, heading, and speed, as well as the pursuer's parameters: position, speed, range, and capture radius. In

contested environments, GPS can be denied, making it difficult for the agent to precisely determine its own parameters. Enemy parameters are often not known precisely; however, the agent may have prior beliefs or estimates of both its own and the enemy's parameters. In this work, we assume that these beliefs take the form of probability distributions.

In this section, we analyze the BEZ model by accounting for uncertainty in both the agent's and pursuer's parameters. We accomplish this through linear covariance analysis and Monte Carlo methods. However, we do not account for the uncertainty in the speed of the agent and the pursuer because this can change if we identify a pursuer as fast $\nu > 1$ or slow $\nu < 1$. The authors in [6] show that the shape of the BEZ differs drastically between the fast and slow pursuer cases. Since we treat the unknown parameters as Gaussian random variables, incorporating speeds would introduce ambiguity regarding whether the scenario involves a fast or slow pursuer, i.e., there would be a non-zero probability (due to the infinite tails of Gaussian distributions) that the pursuer's speed is slower than the agent's, even if the mean pursuer speed is higher. For this reason, we do not evaluate the uncertainty in the speeds, and leave this as an item of future work.

We represent the agent's parameters as $\boldsymbol{\Theta}_A(t) = [\boldsymbol{x}_A(t), \psi_A(t)]^\top$. Because the agent is moving, its parameters may be a function of time; however, the PEZ is only evaluated at the current moment in time and will change when the position or heading of the agent changes. The pursuer's parameters are $\boldsymbol{\Theta}_P = [\boldsymbol{x}_P(0), R, r]^\top$. We do not include the pursuer's heading ψ_P in the parameters because it is not a part of the BEZ equation (the pursuer's heading is assumed to be the optimal collision course heading; this means the BEZ is based off the worst-case heading and therefore provides a conservative safety zone). We assume the parameters are normally distributed $\boldsymbol{\Theta}_A(t) \sim \mathcal{N}(\mu_{\boldsymbol{\Theta}_A}(t), \Sigma_{\boldsymbol{\Theta}_A}(t))$, with

$$\Sigma_{\boldsymbol{\Theta}_A}(t) = \begin{bmatrix} \Sigma_{\boldsymbol{x}_A}(t) & \mathbf{0}_{2\times 1} \\ \mathbf{0}_{1\times 2} & \sigma^2_{\psi_A}(t) \end{bmatrix}, \tag{5}$$

where $\Sigma_{\boldsymbol{x}_A}(t)$ is the covariance of the agent's position, $\sigma^2_{\psi_A}(t)$ is the variance of the agent's heading, and $\Sigma_{\boldsymbol{\Theta}_A}(t) \in \mathbb{R}^{3\times 3}$. If there were a covariance between the agent's position $\boldsymbol{x}_A$ and heading ψ_A, the zero matrices on the off-diagonal would be replaced with those values.

Similarly, we assume the pursuer's parameters are normally distributed $\boldsymbol{\Theta}_P \sim \mathcal{N}(\mu_{\boldsymbol{\Theta}_P}, \Sigma_{\boldsymbol{\Theta}_P})$, with

$$\Sigma_{\boldsymbol{\Theta}_P} = \begin{bmatrix} \Sigma_{\boldsymbol{x}_P(0)} & \mathbf{0}_{2\times 1} & \mathbf{0}_{2\times 1} \\ \mathbf{0}_{1\times 2} & \sigma^2_R & \mathbf{0}_{2\times 1} \\ \mathbf{0}_{1\times 2} & \mathbf{0}_{1\times 2} & \sigma^2_r \end{bmatrix}, \tag{6}$$

where $\Sigma_{\boldsymbol{x}_P(0)}$ is the covariance of the agent's belief of the pursuer's starting location, σ^2_R is the variance of the agent's belief of the range of the pursuer, σ^2_r is the variance of the agent's belief of the pursuer's capture radius, and $\Sigma_{\boldsymbol{\Theta}_P} \in \mathbb{R}^{4\times 4}$. For this work, we assume that these distributions do not change over time, but incorporating changing distributions into this formulation would be a straightforward addition.

To assist with our analysis we define an engagement zone function $z(\boldsymbol{\Theta}_A(t), \boldsymbol{\Theta}_P, \nu)$ as

$$z(\boldsymbol{\Theta}_A(t), \boldsymbol{\Theta}_P, \nu) = \|\boldsymbol{x}_P(0) - \boldsymbol{x}_A\|_2 - \rho(\xi, \nu, R, r). \tag{7}$$

This function is a combination of the distance and Equation (3). When $z(\boldsymbol{\Theta}_A(t), \boldsymbol{\Theta}_P, \nu) \leq 0$ the agent is inside the engagement zone.

Using these equations, we next present the linear covariance method in Section III-A and the MC method in Section III-B. The MC PEZ method generates random samples of the parameter distributions of the pursuer and the agent and propagates them through the engagement zone function (Equation (7)) to account for uncertainty.

A. Linearized Probabilistic Engagement Zone

To find the linearized PEZ we create a linear approximation of the engagement zone function, Equation (7) using a first-order Taylor approximation. To do this, we find the Jacobians of $z(\boldsymbol{\Theta}_A, \boldsymbol{\Theta}_P, \nu)$ with respect to $\boldsymbol{\Theta}_A$ and $\boldsymbol{\Theta}_P$. The first-order approximation is given as

$$\begin{aligned} z(\boldsymbol{\Theta}_A + \boldsymbol{\delta}_A, \boldsymbol{\Theta}_P + \boldsymbol{\delta}_P, \nu) \approx \\ z(\boldsymbol{\Theta}_A, \boldsymbol{\Theta}_P, \nu) + \boldsymbol{\delta}_A \frac{\partial z}{\partial \boldsymbol{\Theta}_A} + \boldsymbol{\delta}_P \frac{\partial z}{\partial \boldsymbol{\Theta}_P}, \end{aligned} \tag{8}$$

where $\partial z / \partial \boldsymbol{\Theta}_A$ is the Jacobian of z with respect to $\boldsymbol{\Theta}_A$ and $\partial z / \partial \boldsymbol{\Theta}_P$ is the Jacobian of z with respect to $\boldsymbol{\Theta}_P$. The Jacobians can be found analytically or through automatic differentiation. In this work, we used the JAX automatic differentiation library [13]. We treat $\boldsymbol{\delta}_A$ and $\boldsymbol{\delta}_P$ as Gaussian random variables with covariances $\Sigma_{\boldsymbol{\Theta}_A}$ and $\Sigma_{\boldsymbol{\Theta}_P}$, respectively. Using this, we can find the approximate mean and covariance of $z(\boldsymbol{\Theta}_A + \boldsymbol{\delta}_A, \boldsymbol{\Theta}_P + \boldsymbol{\delta}_P, \nu)$. This yields a mean of

$$\mu_z(\mu_{\boldsymbol{\Theta}_A}, \mu_{\boldsymbol{\Theta}_P}, \nu) = z(\mu_{\boldsymbol{\Theta}_A}, \mu_{\boldsymbol{\Theta}_P}, \nu), \tag{9}$$

and a covariance of

$$\begin{aligned} \Sigma_z(\mu_{\boldsymbol{\Theta}_A}, \mu_{\boldsymbol{\Theta}_P}, \nu, \Sigma_{\boldsymbol{\Theta}_A}, \Sigma_{\boldsymbol{\Theta}_P}) = \\ \frac{\partial z}{\partial \boldsymbol{\Theta}_A} \Sigma_{\boldsymbol{\Theta}_A} \frac{\partial z}{\partial \boldsymbol{\Theta}_A}^\top + \frac{\partial z}{\partial \boldsymbol{\Theta}_P} \Sigma_{\boldsymbol{\Theta}_P} \frac{\partial z}{\partial \boldsymbol{\Theta}_P}^\top. \end{aligned} \tag{10}$$

Using this approximate distribution, we can now find an approximate probability that the agent is inside the true EZ. This is found as

$$P(z(\boldsymbol{\Theta}_A, \boldsymbol{\Theta}_P, \nu) \leq 0), \tag{11}$$

where

$$z(\boldsymbol{\Theta}_A, \boldsymbol{\Theta}_P, \nu) \dot{\sim} \mathcal{N}(\mu_z, \Sigma_z). \tag{12}$$

This probability can be easily found numerically using the CDF of the multivariate Gaussian distribution. There is a different distribution (μ_f, Σ_f) for each point in which the PEZ is evaluated (for each $\boldsymbol{x}_A$).

B. Monte Carlo Probabilistic Engagement Zone

To evaluate the accuracy of the linearized PEZ, we provide a Monte Carlo (MC) method for comparison. The MC PEZ method relies on random sampling and results in a nonlinear approximation of the PEZ that is more accurate. We draw N_m random samples from the distribution of agent parameters $\overline{\Theta}_A = \{\boldsymbol{\Theta}_A^i\} \sim \mathcal{N}(\mu_{\boldsymbol{\Theta}_A}, \Sigma_{\boldsymbol{\Theta}_A})_{\forall i \in \{1,\dots,N_m\}}$ and N_m samples from the distribution of pursuer parameters $\overline{\Theta}_P = \{\boldsymbol{\Theta}_P^i\} \sim \mathcal{N}(\mu_{\boldsymbol{\Theta}_P}, \Sigma_{\boldsymbol{\Theta}_P})_{\forall i \in \{1,\dots,N_m\}}$. We then propagate the random samples through $z(\boldsymbol{\Theta}_A, \boldsymbol{\Theta}_P, \nu)$ to give

$$\overline{Z} = \{z(\boldsymbol{\Theta}_A^i, \boldsymbol{\Theta}_P^i, \nu)\}_{\forall \boldsymbol{\Theta}_A^i \in \overline{\Theta}_A, \boldsymbol{\Theta}_P^i \in \overline{\Theta}_P}. \tag{13}$$

We can approximate $P(z(\boldsymbol{\Theta}_A, \boldsymbol{\Theta}_P, \nu) \leq 0)$ by counting the number of elements of $\overline{Z}$ that are less then zero,

$$P(z(\boldsymbol{\Theta}_A, \boldsymbol{\Theta}_P, \nu) \leq 0) \approx \frac{1}{N_m} \sum_{z^i \in \overline{Z}} \mathbb{1}(-z^i) \tag{14}$$

where $\mathbb{1}(z)$ is an indicator function defined as

$$\mathbb{1}(z) = \left\{ \begin{array}{ll} 0 & z < 0 \\ 1 & z \geq 0 \end{array} \right\}. \tag{15}$$

This counts the number of samples of $\overline{Z}$ less than 0 and then divides by the number of samples, approximating the true probability of being inside the EZ, given the distributions of the agent and pursuer parameters. As the number of samples N_m increases, this approximation improves. We use the MC PEZ as a comparison for the linearized PEZ. In practice, especially for path planning, evaluating the MC PEZ is too expensive for real-time performance.

IV. Path Optimization using PEZ

To illustrate the usefulness of the linearized PEZ formulation, we now present the path optimization approach using linearized PEZ. When traversing contested environments, agents need safe paths that avoid adversaries while accounting for uncertainty in their self-knowledge and adversarial knowledge. Past work in [4] and [3] used a different EZ definition to plan safe minimum-time trajectories around EZs. The authors in [6] use the BEZ formulation to plan conflict-free paths around the pursuers, paths that do not require the agent to take evasive maneuvers to avoid being captured. In this work, we present a similar path planning scheme; however, we use linearized PEZs, accounting for uncertainty in the pursuer's parameters.

Due to their ability to efficiently parameterize paths, we use B-splines as our representation. B-splines are defined by a list of control points $\overline{C} = (\boldsymbol{c}_1, \boldsymbol{c}_2, \dots, \boldsymbol{c}_{N_c})$, where N_c is the number of control points, and knot points $\boldsymbol{t}_k = (t_0 - k\Delta_t, \dots, t_0 - \Delta_t, t_0, t_0 + \Delta_t, \dots, t_f, t_f + \Delta_t, \dots, t_f + k\Delta_t)$, where t_0 is the starting time of the trajectory, t_f is the final time of the trajectory, k is the order of the B-spline, $\Delta_t = (t_f - t_0)/N_k$ is the time spacing of the knot points, and N_k is the number of internal knot points. Using the knot points to define basis functions, a B-spline trajectory is defined as

$$\boldsymbol{p}(t) = \sum_{i=1}^{N_c} B_{i,k}(t)\boldsymbol{c}_i, \tag{16}$$

where the basis function $B_{i,k}(t)$ are defined using the Cox-de Boor recursive formula shown in [14]. B-splines are useful for path planning because the basis functions have finite support (changing control points at the beginning of the spline does not effect the end), and they can be easily differentiated.

The goal of the path planner is to find the minimum time trajectory that starts at $\boldsymbol{x}_A(0)$ and ends at $\boldsymbol{x}_A(t_f)$, while also using the linearized PEZ to ensure that the probability of the agent entering the EZ is below a threshold. We also include constraints that ensure the path is kinematically feasible, similar to our previous work [15]. This yields an optimization problem of

$$\overline{C}_{opt}, t_{f_{opt}} = \underset{\overline{C}, t_f}{\operatorname{argmin}}\, t_f \tag{17a}$$

$$\text{subject to } \boldsymbol{p}(0) = \boldsymbol{x}_A(0) \tag{17b}$$

$$\boldsymbol{p}(t_f) = \boldsymbol{x}_A(t_f) \tag{17c}$$

$$\boldsymbol{p}(\boldsymbol{t}_s) \in \mathcal{D} \tag{17d}$$

$$P(z(\boldsymbol{\Theta}_A(\boldsymbol{t}_s), \boldsymbol{\Theta}_P, \nu) \leq 0) \leq \epsilon \tag{17e}$$

$$v(\boldsymbol{t}_s) = v_A \tag{17f}$$

$$u_{lb} \leq u_A(\boldsymbol{t}_s) \leq u_{ub} \tag{17g}$$

$$-\kappa_{ub} \leq \kappa_A(\boldsymbol{t}_s) \leq \kappa_{ub}, \tag{17h}$$

where u_{lb} and u_{ub} are the lower and upper turn-rate constraints, κ_{ub} is the path curvature constraint and $u_A(t)$ and $\kappa_A(t)$ are the turn rate and curvature of the trajectory. The constraints must be discretely sampled, $\boldsymbol{t}_s = \{0, \Delta_s, 2\Delta_s, \dots, t_f\}$, $\Delta_s = t_f/N_s$, where N_s is the number of discrete constraint samples. The first and second constraints (Equations (17b) and (17c)) ensure that the path starts at the agent's initial position and finishes at the goal. The next constraint (Equation (17d)) ensures that the agent remains within the operating region $\mathcal{D}$. Equation (17e) is the PEZ constraint (17e) that ensures that the approximate probability of being inside the true engagement zone remains below a threshold ϵ. The next three constraints (Equations (17f)- (17h)) ensure kinematic feasibility in velocity, turn rate, and curvature. The velocity of the trajectory can be found as $v(t) = ||\dot{\boldsymbol{p}}(t)||_2$. The turn rate is $u(t) = (\dot{\boldsymbol{p}}(t) \times \ddot{\boldsymbol{p}}(t))/||\dot{\boldsymbol{p}}(t)||_2^2$. The final kinematic constraint is the curvature and can be found as $\kappa(t) = u(t)/v(t)$.

We use a gradient-based interior point optimization algorithm called IPOPT [16]. Because it is a gradient-based method, the gradient of the objective function as well as Jacobians of the constraints are needed. We use the JAX automatic differentiation library to find this gradient and Jacobians [13].

V. Results

In this section, we present results demonstrating the effectiveness of using the linearized PEZ in our path-planning algorithm. To validate the linearized PEZ, we first compare it with Monte Carlo (MC) PEZs. Subsequently, we provide results for path planning that utilize linearized PEZs and compare these results with those obtained using deterministic BEZs.

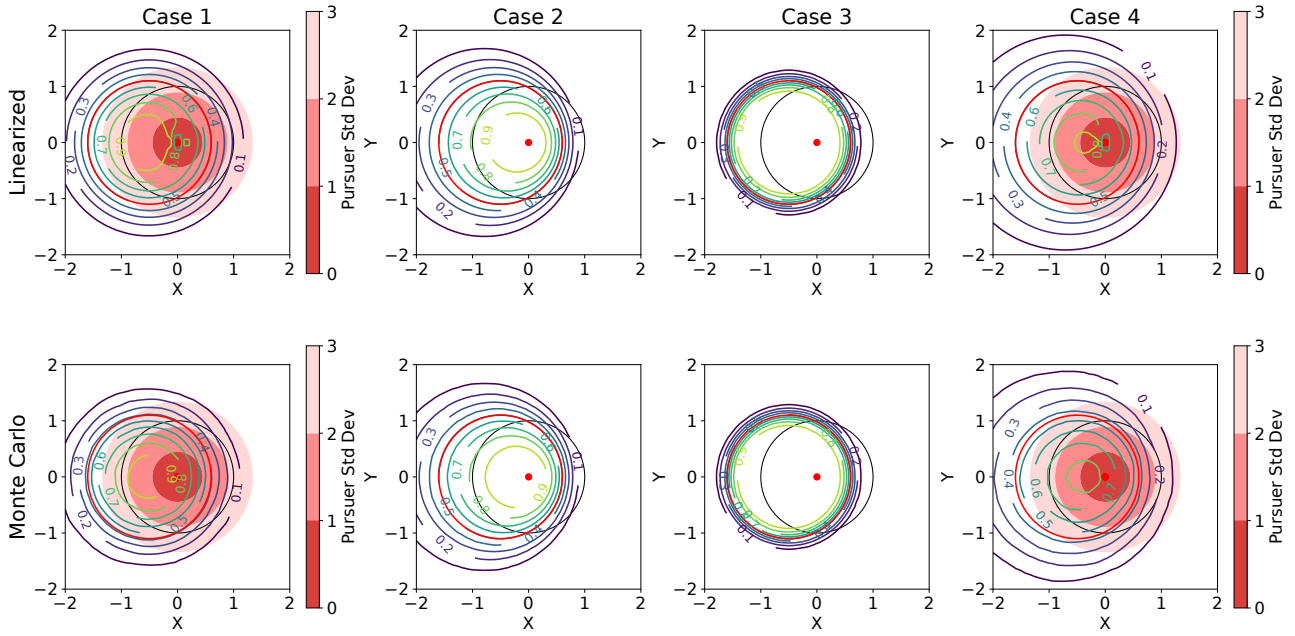

Fig. 2. This figure shows the linearized and MC PEZ for 4 cases. The black circles show the pursuer's range. The red circles show the deterministic BEZ and the colored circles show the level sets of probability of being inside the true EZ for both the linearized PEZ and the MC PEZ. The red point is the mean value of the initial position of the pursuer ($\boldsymbol{x}_{P_0}$). The 3-sigma bounds of the pursuer's initial location are shown in the filled red circles.

TABLE I

RMSE BETWEEN LINEARIZED PEZ AND MONTE CARLO PEZ FOR DIFFERENT UNCERTAINTY LEVELS.

	$\mu_{\boldsymbol{x}_A}$	$\Sigma_{\boldsymbol{x}_A}$	μ_{ψ_A}	$\sigma^2_{\psi_A}$	$\mu_{\boldsymbol{x}_P}$	$\Sigma_{\boldsymbol{x}_P}$	μ_R	σ^2_R	μ_r	σ^2_r	v_P	v_A	RMSE
Case 1	-	$\begin{bmatrix}0.0 & 0.0\\ 0.0 & 0.0\end{bmatrix}$	-	0	$\begin{bmatrix}0.0\\ 0.0\end{bmatrix}$	$\begin{bmatrix}0.2 & 0.0\\ 0.0 & 0.2\end{bmatrix}$	1.0	0.0	0.1	0.0	1.0	0.5	0.0474
Case 2	-	$\begin{bmatrix}0.0 & 0.0\\ 0.0 & 0.0\end{bmatrix}$	-	0	$\begin{bmatrix}0.0\\ 0.0\end{bmatrix}$	$\begin{bmatrix}0.0 & 0.0\\ 0.0 & 0.0\end{bmatrix}$	1.0	0.2	0.1	0.0	1.0	0.5	0.0480
Case 3	-	$\begin{bmatrix}0.0 & 0.0\\ 0.0 & 0.0\end{bmatrix}$	-	0	$\begin{bmatrix}0.0\\ 0.0\end{bmatrix}$	$\begin{bmatrix}0.0 & 0.0\\ 0.0 & 0.0\end{bmatrix}$	1.0	0.0	0.1	0.02	1.0	0.5	0.0482
Case 4	-	$\begin{bmatrix}0.0 & 0.0\\ 0.0 & 0.0\end{bmatrix}$	-	0	$\begin{bmatrix}0.0\\ 0.0\end{bmatrix}$	$\begin{bmatrix}0.2 & 0.0\\ 0.0 & 0.2\end{bmatrix}$	1.0	0.2	0.1	0.02	1.0	0.5	0.0468
Case 5	-	$\begin{bmatrix}0.2 & 0.0\\ 0.0 & 0.2\end{bmatrix}$	-	0	$\begin{bmatrix}0.0\\ 0.0\end{bmatrix}$	$\begin{bmatrix}0.0 & 0.0\\ 0.0 & 0.0\end{bmatrix}$	1.0	0.0	0.1	0.00	1.0	0.5	0.0472
Case 6	-	$\begin{bmatrix}0.0 & 0.0\\ 0.0 & 0.0\end{bmatrix}$	-	0.2	$\begin{bmatrix}0.0\\ 0.0\end{bmatrix}$	$\begin{bmatrix}0.0 & 0.0\\ 0.0 & 0.0\end{bmatrix}$	1.0	0.0	0.1	0.00	1.0	0.5	0.0552
Case 7	-	$\begin{bmatrix}0.2 & 0.0\\ 0.0 & 0.2\end{bmatrix}$	-	0.2	$\begin{bmatrix}0.0\\ 0.0\end{bmatrix}$	$\begin{bmatrix}0.2 & 0.0\\ 0.0 & 0.2\end{bmatrix}$	1.0	0.2	0.1	0.02	1.0	0.5	0.0793

Table I shows seven different cases with varying parameters that we used to test the linearized PEZ. Our values are shown as unitless because this method can be used for a variety of vehicles with arbitrary speeds, ranges, and capture radii. The ratio of these parameters is what matters. So, showing the cases where $\nu = 0.5$, we represent situations where the pursuer is twice as fast as the agent. The first four cases show uncertainty in the pursuer parameters $\boldsymbol{\Theta}_P$. Cases 1-3 isolate each parameter, and Case 4 shows the combined effect. Cases 5 and 6 show uncertainty only in the agent's parameters $\boldsymbol{\Theta}_A$. And the final case shows uncertainty in both agent and pursuer parameters. We report the RMSE between the linearized PEZ and the MC PEZ. This is computed by evaluating the linearized PEZ and the MC PEZ on a grid of points and then computing the RMSE between the values at those points. From this comparison, we see that the agent's heading (Case 6) ψ_A has the greatest effect on the accuracy of the linearized PEZ. The RMSE is reasonable for all cases showing that the linearized PEZ model is a useful approximation.

Figure 2 shows the linearized PEZ and MC PEZ for the first four cases. The levels of the probability of being inside the true BEZ ($P(f(\boldsymbol{\Theta}_A, \boldsymbol{\Theta}_P, \nu) \leq 0)$) are shown. From the figure, it is apparent that the linearized PEZ is approximately the same as the MC PEZ. The deterministic BEZ is colored red. The BEZ corresponds to the 50% level of the linearized PEZ.

Next, we show simulation results for the PEZ path planner. We evaluate the path planner for the first four cases as shown in Table I. We only show the cases where the agent's parameters are known precisely and where the pursuer's parameters are uncertain. Our method would work in cases where there is uncertainty in the agent's parameters; however, to realistically apply this situation, the agent's parameter

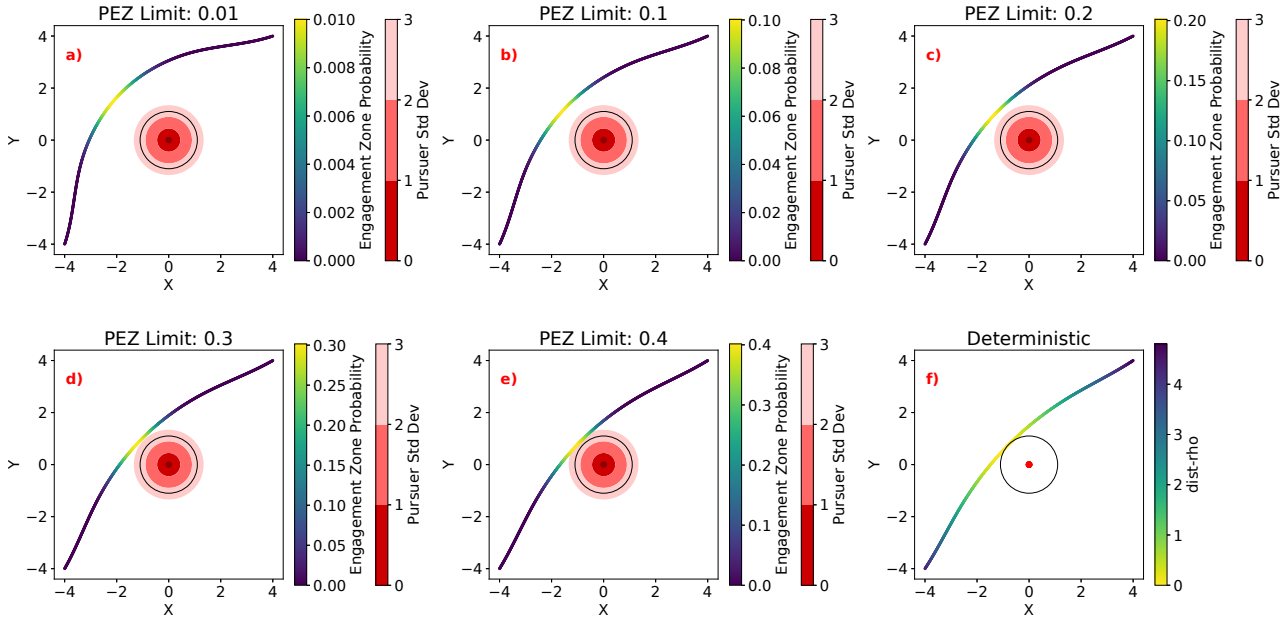

Fig. 3. Six different paths are shown. The mean value of the pursuer's location is shown as a red point, and 3-sigma bounds are shown as solid red circles. The black circle shows the range of the pursuer. For a-e, the color of the path indicates the linearized PEZ at that point on the path. For f, the color shows z the BEZ constraint, the closer to 0 the closer the trajectory is to being inside the BEZ. The lower the PEZ limit, the further the path has to go to maintain the constraint. These paths were all planned using the parameters in Case 4 and different linearized PEZ thresholds.

uncertainty would need to vary as the agent moves. An extended Kalman filter (EKF) could be used to track the agent's parameters and their uncertainty as was done in [11]. However, integrating an EKF for agent state estimation and our path planner is beyond the scope of this conference paper, and we leave it for future work.

For all cases, the agent started at $x_A(0) = [-4, -4]^\top$ and had a goal of $x_A(t_f) = [4, 4]^\top$. We planned the agent's path using a third-order spline $k = 3$ with $N_c = 7$ and $N_s = 100$.

Figure 3 shows the optimized trajectories using the formulation in Equation (17) and the parameters in Case 4 from Table I. The figure shows five planned paths using the PEZ constraint and one planned path using the BEZ constraint. The lower the value of the PEZ constraint ϵ the wider the path must deviate to avoid the pursuer. The BEZ constrained path (deterministic) takes the tightest route. Because the mean value of z corresponds to the BEZ constraint, using the BEZ constraint is equivalent to using $\epsilon = 0.5$. We only show values of $\epsilon \leq 0.5$, because values greater than 0.5 would be equivalent to planning paths that are more likely than not to be in the true EZ. For example, a PEZ limit of $\epsilon = 0.01$ corresponds to a constraint that the path must not exceed a 1% probability of being within the true EZ.

Table II shows the results for different planned paths using the parameters shown in Cases 1-4 of Table I. The Case 4 paths in this table correspond to the planned paths shown in Figure 3. The table shows the linearized PEZ threshold, the planned path time t_f, and the MC probability that the path violates the true BEZ. To compute the MC probability of the path violating the true BEZ, a path was planned for each threshold. After the path was planned, N_m samples were drawn from the distribution of pursuer parameters $\mathbf{\Theta}_P$. Using the sampled parameter, we evaluated points along the trajectory to see if they violated the deterministic BEZ created from each sample. The number of these violations was counted and then divided by the total number of MC runs. This provides a metric to show how well the linearized PEZ performed. Ideally, if the linearization exactly approximated the true BEZ, the linearized PEZ threshold and MC probability would be the same. However, from Table II, we see that there is some disparity due to linearization errors. The difference between the linearized PEZ and the MC probability is small. In general, Case 4 shows the greatest disparity between the linearized PEZ and the MC evaluation. However, the linearized PEZ threshold and the MC evaluation match very closely.

These results show the usefulness of the linearized PEZ. For a small increase in total path time (22.69 versus 24.89 seconds), there is a significant increase in safety (ranging from a 50.65% chance of being inside the true BEZ to around a 1.33% chance). When there is uncertainty in the parameters of the purser, the linearized PEZ formulation can be favorable to account for this uncertainty and maintain safe paths.

VI. Conclusion

In this work, we present a method that extends past work on EZs to account for uncertainty in pursuer parameters and agent (evader) parameters. We specifically account for uncertainty in the location, range, and capture radius of the pursuer and the position and heading of the agent in the evader/pursuer differential game. We do this through a linearized PEZ method that linearly approximates the BEZ

TABLE II

THIS TABLE SHOWS THE PATH LENGTH IN SECONDS AND THE MC PROBABILITY THAT THE PLANNED PATH VIOLATES THE TRUE BEZ.

PEZ Thresh (ϵ)	Case 1		Case 2		Case 3		Case 4	
	t_f	MC prob	t_f	MC prob	t_f	MC prob	t_f	MC prob
0.01	24.05	0.0122	24.03	0.0114	23.04	0.0093	24.89	0.0133
0.05	23.57	0.0582	23.56	0.0533	22.92	0.0507	24.08	0.0562
0.1	23.34	0.1082	23.34	0.1024	22.86	0.0981	23.70	0.1081
0.2	23.09	0.2050	23.09	0.2022	22.80	0.2018	23.30	0.2138
0.3	22.92	0.3089	22.92	0.3118	22.76	0.3045	23.04	0.3072
0.4	22.78	0.4191	22.80	0.4030	22.72	0.4019	22.84	0.4100
Deterministic	22.69	0.5087	22.69	0.5006	22.69	0.4987	22.69	0.5065

equations and propagates the uncertainty through them. We provide an MC PEZ comparison that is computationally more expensive but better approximates the true PEZ. This comparison showed that the linearized PEZ is a sufficient approximation of the MC PEZ. We also provide a method for using the linearized PEZ to plan safe paths that show a significant improvement in safety when compared to a standard BEZ under uncertainty in the pursuer's parameters.

Future work includes improving the linearized approximation; this could be done using improved uncertainty propagation, such as with an unscented transform. Uncertainty in the speed of the agent and pursuer also needs to be taken into account. Path planning with uncertainty in the agent's position and heading also provides an interesting area of research, especially considering the prevalence of GPS-denied regions in contested environments.

REFERENCES

[1] M. Jun and R. D'Andrea, "Path planning for unmanned aerial vehicles in uncertain and adversarial environments," *Cooperative control: models, applications and algorithms*, pp. 95–110, 2003.

[2] X. Peng and D. Xu, "Intelligent online path planning for uavs in adversarial environments," *International Journal of Advanced Robotic Systems*, vol. 9, no. 1, p. 3, 2012.

[3] I. E. Weintraub, A. Von Moll, C. A. Carrizales, N. Hanlon, and Z. E. Fuchs, "An optimal engagement zone avoidance scenario in 2-D," in *AIAA SCITECH 2022 Forum*, p. 1587, 2022.

[4] P. M. Dillon, M. D. Zollars, I. E. Weintraub, and A. Von Moll, "Optimal trajectories for aircraft avoidance of multiple weapon engagement zones," *Journal of Aerospace Information Systems*, vol. 20, no. 8, pp. 520–525, 2023.

[5] A. Wolek, I. E. Weintraub, A. Von Moll, D. Casbeer, and S. G. Manyam, "Sampling-based risk-aware path planning around dynamic engagement zones," *arXiv preprint arXiv:2403.05480*, 2024.

[6] A. Von Moll and I. Weintraub, "Basic engagement zones," *Journal of Aerospace Information Systems*, pp. 1–7, 2024.

[7] R. Isaacs, "Differential games, a mathematical theory with applications to optimization," 1965.

[8] I. E. Weintraub, M. Pachter, and E. Garcia, "An introduction to pursuit-evasion differential games," in *2020 American Control Conference (ACC)*, pp. 1049–1066, 2020.

[9] A. Friedman, "Stochastic differential games," *Journal of differential equations*, vol. 11, no. 1, pp. 79–108, 1972.

[10] A. Patil, Y. Zhou, D. Fridovich-Keil, and T. Tanaka, "Risk-minimizing two-player zero-sum stochastic differential game via path integral control," in *2023 62nd IEEE Conference on Decision and Control (CDC)*, pp. 3095–3101, IEEE, 2023.

[11] A. Costley, G. Droge, R. Christensen, R. C. Leishman, and J. Swedeen, "Path planning with uncertainty for aircraft under threat of detection from ground-based radar," *arXiv preprint arXiv:2207.03716*, 2022.

[12] A. Costley, R. S. Christensen, R. C. Leishman, and G. N. Droge, "Sensitivity of the probability of radar detection to radar state uncertainty," *IEEE Transactions on Aerospace and Electronic Systems*, vol. 59, no. 6, pp. 9740–9747, 2023.

[13] J. Bradbury, R. Frostig, P. Hawkins, M. J. Johnson, C. Leary, D. Maclaurin, G. Necula, A. Paszke, J. VanderPlas, S. Wanderman-Milne, and Q. Zhang, "JAX: composable transformations of Python+NumPy programs," 2018.

[14] M. G. Cox, "The numerical evaluation of B-splines," *IMA Journal of Applied mathematics*, vol. 10, no. 2, pp. 134–149, 1972.

[15] G. Stagg and C. K. Peterson, "Multi-agent path planning for level set estimation using B-splines and differential flatness," *IEEE Robotics and Automation Letters*, 2024.

[16] A. Wächter and L. T. Biegler, "On the implementation of an interior-point filter line-search algorithm for large-scale nonlinear programming," *Mathematical programming*, vol. 106, no. 1, pp. 25–57, 2006.